2006-08-08

Influence of ECAP processing parameters on texture and microstructure of commercially pure aluminum

Zhilyaev, A. P.; Oh-ishi, K.; Raab, G. I.; McNelley, T. R.

Elsevier

Materials Science and Engineering a, v. 441, 2006, pp. 245-252
https://hdl.handle.net/10945/43163

ELSEVIER

Materials Science and Engineering A 441 (2006) 245–252

MATERIALS SCIENCE & ENGINEERING A

www.elsevier.com/locate/msea

Influence of ECAP processing parameters on texture and microstructure of commercially pure aluminum

A.P. Zhilyaev [a,*,1], K. Oh-ishi [a,2], G.I. Raab [b], T.R. McNelley [a]

[a] *Department of Mechanical and Astronautical Engineering, Naval Postgraduate School, Monterey, CA 93943, USA*

[b] *Institute for Physics of Advanced Materials, USATU, 450001 Ufa, Russia*

Received 10 May 2006; received in revised form 3 August 2006; accepted 8 August 2006

Abstract

The development of shear textures and band-like features in the microstructure of commercially pure (CP) aluminum have been studied as a function of backpressure and die relief angle during equal-channel angular pressing (ECAP) through a die with a 90° die channel angle. Microtexture data were acquired by orientation imaging microscopy (OIM) following one pass and four repetitive passes by route A. In a 90° die with zero relief angle, the microtexture data indicate that ECAP involves simple shear on a shear plane and in a shear direction that are rotated away from the plane of the die channel intersection toward the die exit channel. This rotation reflects the spreading of shear deformation through a fan-shaped region around the plane of the die channel intersection. The superposition of backpressure suppresses this spreading and the texture data indicate that deformation is confined to the plane of the die channel intersection, while the introduction of a relief angle at the outer corner of the die channel intersection promotes spreading and leads to further rotation of the shear plane and shear direction toward the axis of the die exit channel. Splitting of shear texture components is observed after the initial ECAP pass. Such splitting appears in the microstructure as band-like features separated by sub-grains. Band-like features became apparent in the microstructure after the initial pass and persisted through four ECAP passes by route A; these features become more prominent with increasing die relief angle.

Keywords: Aluminum; Equal channel angular pressing (ECAP); Texture; Simple shear; Orientation imaging microscopy (OIM)

1. Introduction

ECAP is a promising process for the production of ultrafine-grained (UFG) structures in bulk material because the procedure may be applied repeatedly to a billet without changing its cross-section [1]. Large strains and UFG structures may be achieved by high-pressure torsion (HPT) [2] but the method is restricted to small samples while accumulative roll-bonding (ARB) [3] must involve reduction in cross-section in order to achieve effective bonding. The applicability of still other methods to bulk material, such as friction stir processing (FSP) [4], must still be established.

Although the first publications on ECAP appeared almost 25 years ago [5] there has been a surge of interest over the last decade in the development of UFG structures in pure metals and alloys by this method. A survey of the literature reveals that most publications have been concerned with the capability of ECAP to produce highly refined grains in a range of pure metals and alloys, and the roles of ECAP parameters (die channel angle, the number of pressing passes, billet rotation between passes and relief angles in the die) in grain refinement have been of primary interest. In general, microstructure refinement and texture evolution during ECAP have been studied separately and few systematic investigations have been conducted on the concomitant development of texture and microstructure.

Among various factors backpressure as well as die relief angle have been shown to influence the evolution of microstructure and texture during ECAP [6]. For example, the application of back-

* Corresponding author. Present address: Centro Nacional de Investigaciones Metalúrgicas (CENIM-CSIS), Avda. Gregorio del Amo, 8, 28040 Madrid, Spain. Fax: +34 91 534 7425.

E-mail address: AlexZ@anrb.ru (A.P. Zhilyaev).

[1] On leave from Institute for Metals Superplasticity Problems, Russian Academy of Science, 450001 Ufa, Russia.

[2] Present address: National Institute of Materials Science, 1-2-1 Sengen, Tsukuba 305-0047, Japan.

0921-5093/$ – see front matter © 2006 Elsevier B.V. All rights reserved.
doi:10.1016/j.msea.2006.08.029

pressure during ECAP retards cracking of intermetallic particles and enhances the workability and ductility of materials, such as AA5083 and Al–5 wt.% Fe [7]. In fact, any ECAP billet processed by more than one pass experiences some backpressure as it moves into the exit channel of the die.

Band-like arrangements of characteristic shear texture orientations have been observed in the microstructure of pure aluminum processed by repetitive ECAP using a 90° die that also included a 20° relief angle at the outer corner of the die channel intersection [8]. In the idealized description of ECAP simple shear occurs on the plane of the die channel intersection, which is perpendicular to the flow plane, and in the direction of the *bisector of the die angle*. However, recent texture measurements after one ECAP pass through a 90° die for pure aluminum [9] and for pure copper [10] have indicated that simple shear tends to occur on a plane and in a direction that are rotated significantly away from the plane of the die channel intersection toward the die exit channel.

In the present work, microtexture data have been acquired by OIM from large areas along the centerline of CP aluminum billets that have been processed by one ECAP pass, as well as billets following four repetitive passes by route A. The pressing was accomplished in a die designed to allow pressing either with or without backpressure as well as to allow the variation of the die relief angle. Then, the objective of this work is to determine the separate effects of backpressure and die relief angle on texture and microstructure development during an initial ECAP pass and after four repetitive pressing pass by route A.

2. Experimental material and procedure

A CP aluminum (99.7%) plate was machined to provide 8 mm × 8 mm × 50 mm billets for pressing in a 90° die. Prior to ECAP, the billets were annealed. From conventional optical microscopy the initial, recrystallized grain size was ~0.2 mm [11]. ECAP of the square billets was conducted at room temperature using a die with an angle, Φ, between channels of 90° as illustrated in schematics of Fig. 1. The introduction of die relief results in shearing perpendicular to as well as parallel to the plane of the die channel intersection. Here, inserts allowed pressing with relief angles, Ψ, of 0°, 45°, or 90°, and the die geometry as well as influence of relief angle on shear are shown schematically in Fig. 1(a–c) for these angles, respectively. Axis systems for the description of the strain are indicated in Fig. 1(d). A billet inserted into an empty die channel will not experience back pressure as it passes through the die channel intersection during pressing. In contrast, a second billet inserted immediately behind the initial billet will experience a backpressure on the order of the flow stress of the CP aluminum. Two such billets are shown Fig. 1(e); the billet on the right-hand side was first through the die and did not experience back pressure while the billet on the left-hand side was pressed with the first in place and, so, experienced back pressure.

Samples for OIM were mechanically polished and then electropolished in a Buehler Electromet 4 apparatus using a 20% perchloric acid–80% ethanol electrolyte cooled to −25 °C. The OIM utilized a Topcon S510 scanning electron microscope operating with a tungsten filament. The minimum step size of 0.1 μm was no more than about 0.1 of the mean (sub)grain size in these materials. Samples were always examined at the center of ECAP flow plane in order to avoid die wall effects. The symmetry of an ECAP billet is monoclinic, and so the senses of the coordinate axes in the flow plane were carefully ascertained. The OIM study involved standard clean-up procedures [12], as follows: (i) grain dilatation with a grain tolerance angle (GTA) of 5°; a minimum grain size (MGS) of two pixels; (ii) grain confidence index (CI) standardization with GTA = 5° and MGS = 2; (iii) neighbor CI correlation with minimum CI of 0.1. The result of applying such a clean-up procedure is shown in Fig. 2 for annealed and unpressed material. The grains are separated by thick lines (high-angle boundaries of 15–62.8°) or thin lines (low-angle boundaries of 5–15°). Here, the mean grain size (grain diameter) is about 33.5 μm, a value which is about one order magnitude finer than that measured by optical microscopy. Conventional

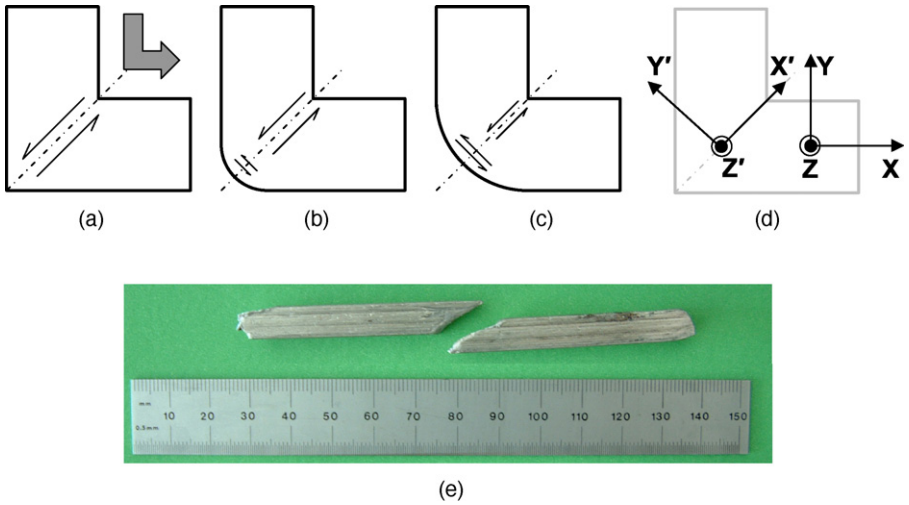

Fig. 1. Schematics of ECAP pressing (in the flow plane) using die relief angles, Ψ, of: (a) 0°; (b) 45°; (c) 90°; axis systems for description of resulting shear textures are shown in (d). Billet appearance after one pass through the ECAP die with (left) and without (right) back pressure is shown in (e).

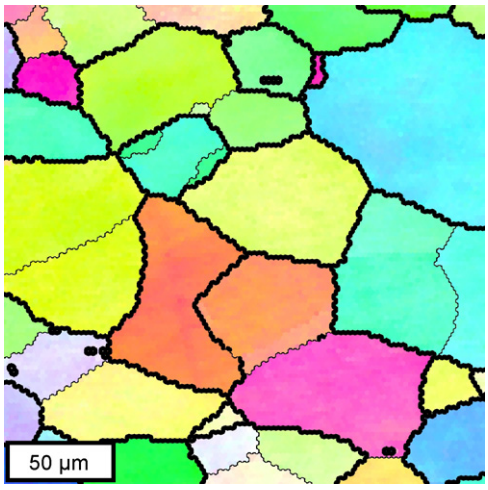

Fig. 2. The microstructure of unpressed CP aluminum by OIM; heavy lines correspond to high-angle boundaries of 15–62.8° disorientation; light lines are boundaries of 5–15° disorientation.

transmission electron microscopy (TEM) was conducted on selected samples in this study and details of sample preparation and observation have been given previously [13].

3. Results

The orientation data acquired by conventional OIM has high spatial resolution in a small region of the material. Thus, textures obtained by this method after the early stages of ECAP of CP aluminum typically exhibit a few prominent orientations [8–11,13] rather than continuous distributions along shear texture orientation fibers [14,15]. The orientation fibers are the A fiber, which is $\{1\,1\,1\}\langle u\,v\,w\rangle$ (the notation refers to {plane parallel to the shear plane}⟨direction parallel to the shear direction⟩), and the B fiber, which is $\{h\,k\,l\}\langle 1\,1\,0\rangle$. The C orientation, $\{1\,0\,0\}\langle 1\,1\,0\rangle$, lies at one end of the B fiber. In order to assist in interpretation of textures in this investigation pole figures were plotted for four of the prominent orientations that are frequently observed in ECAP of CP aluminum. These are illustrated in Fig. 3(a) by $\{1\,1\,1\}$ pole figures corresponding to the shear plane for simple shear ($X'Z'$ in Fig. 1); these same orientations have been rotated by 90° about the shear direction (SD; X' in Fig. 1) to correspond to the flow plane for simple shear in Fig. 3(b). Finally, these orientations have been rotated by 45° about the flow plane normal (Z in Fig. 1) so that the SD coincides with the location of the bisector of the die channel angle for pressing in a 90° die. These four prominent orientations are an A fiber orientation, $\{1\,1\,1\}\langle 1\,1\,2\rangle$; the orientation at the intersection of the A and B fibers, $\{1\,1\,1\}\langle 1\,1\,0\rangle$, that is designated here as A/B; a B fiber orientation $\{1\,1\,2\}\langle 1\,1\,0\rangle$; and the C orientation. Finally, the A, A/B and B orientations in Fig. 3 each have two crystallographically distinct variants. The pole figures in Fig. 3(c) may be used as keys in analyzing orientations observed in ECAP billets.

Textures and microstructures are inhomogeneous after the initial ECAP pass and representative examples have been chosen here. Inverse pole figure (IPF) maps and discrete $\{1\,1\,1\}$

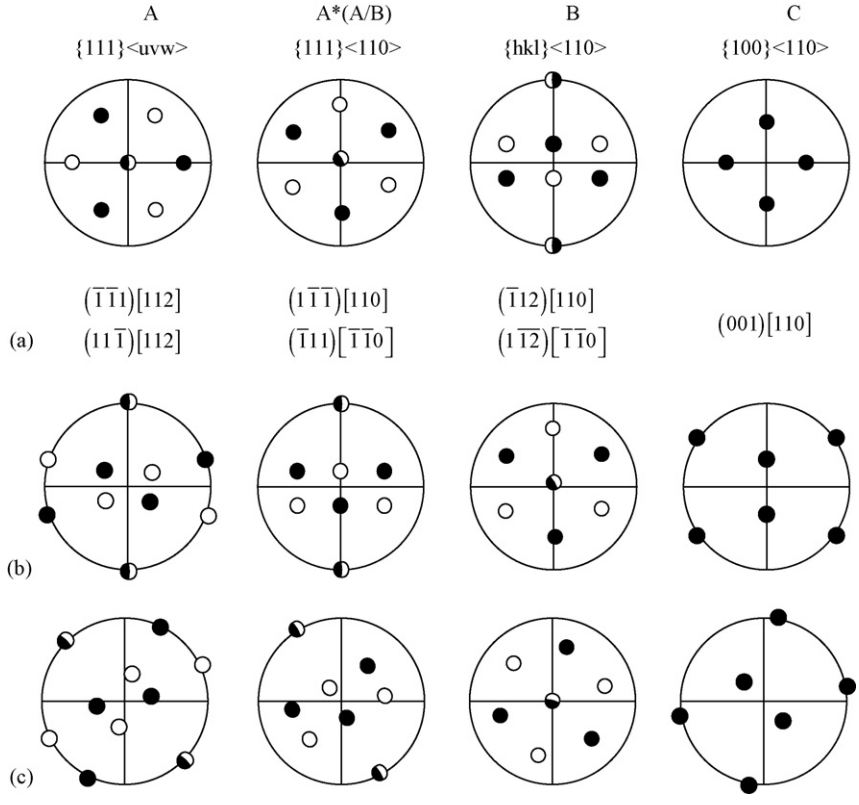

Fig. 3. (1 1 1) pole figures and Miller indices of selected simple shear texture components viewed in different planes: (a) in plane $X'Z'$, (b) in plane $X'Y'$, (c) in plane XY; the axis systems are as defined in Fig. 1.

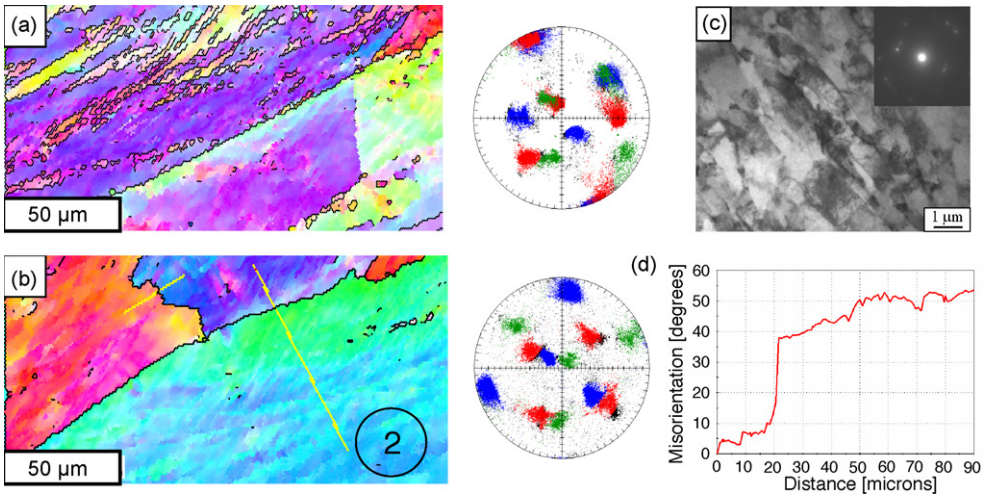

Fig. 4. Inverse pole figure (IPF) color map and (1 1 1) pole figures (PFs) from the flow plane (Fig. 1) after one ECAP pass ($\Psi = 0^\circ$) without (a) and with (b) backpressure. Bright-field TEM micrograph from the flow plane (negative side of the view in Fig. 1) of the sample (b) is shown in (c). A point-to-origin misorientation traverse along line 2 in (b) is shown in (d).

pole figures for aluminum pressed with $\Psi = 0^\circ$ are shown in Fig. 4. The colors will appear as a gray scale in a printed version of this paper. The data in Fig. 4(a) are for the first billet, pressed without backpressure, and in Fig. 4(b) are for the second billet, which experienced backpressure during pressing. These microstructures and textures are represented in the flow plane of the ECAP die, i.e., as illustrated in the schematic of Fig. 1(a). Comparison of the pole figure data in Fig. 4(a) to the idealized ECAP shear texture components in Fig. 3(c) reveals that the experimental texture consists of two variants of the A/B orientation, $\{1\,1\,1\}\langle 1\,1\,0\rangle$ [14,15], that are rotated by 20–25° about the flow normal toward the axis of die exit channel. A high-angle boundary apparently separates these texture variants in the material. Two variants of a B fiber orientation, $\{1\,1\,2\}\langle 1\,1\,0\rangle$, may be identified in the sample pressed with back pressure. In Fig. 4(b) these variants appear to be rotated about the SD; however, the SD is aligned with the bisector of the die channel angle and, so, these texture components are nearly aligned with the idealized shear plane of the ECAP die. Careful examination reveals a splitting by about 5° in both B fibers; this is particularly the case for the 'green' orientation. Such splitting will be noted for die relief angles of 45 and 90° as well. Fig. 4(c) is a bright-field TEM micrograph from the negative side of the flow plane of the sample in Fig. 4(b) and shows refined subgrains ~1 μm in thickness and 2–3 μm in length along the shear direction. Such a structure is typical of CP aluminum following ECAP (see, e.g., [13]). A representative point-to-origin disorientation traverse is shown in Fig. 4(d); such traverses indicate that there are long-range lattice rotations in the microstructure, especially near boundaries, and that high-angle boundaries are frequently interfaces between shear texture variants.

A similar study was performed on materials pressed through a die having a 45° relief angle and results are summarized in Fig. 5. The introduction of this die relief angle, which introduces shearing progressively through a fan-shaped region surrounding the plane of the die channel intersection, apparently has had a limited effect on the resulting textures. An A/B component that is aligned with the plane of the die channel intersection may

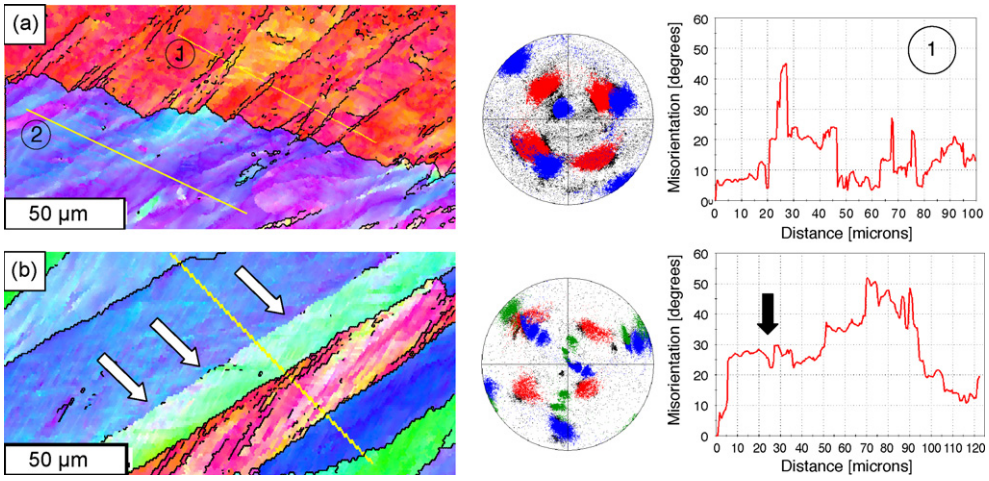

Fig. 5. IPF color map, (1 1 1) PFs and misorientation traverse along line for ECAP ($\Psi = 45^\circ$) of CP aluminum without (a) and with (b) backpressure.

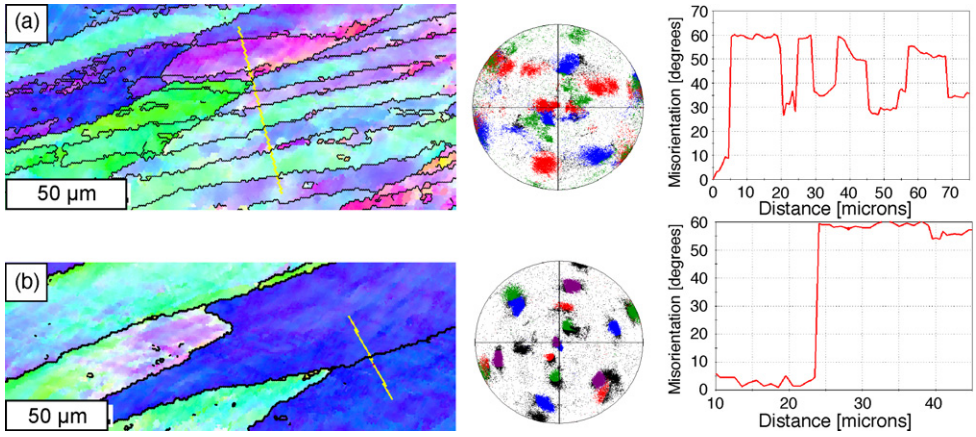

Fig. 6. IPF color map, (1 1 1) PFs and misorientation traverse along line for ECAP ($\Psi = 90^\circ$) of CP aluminum without (a) and with (b) backpressure. Disorientation traverses are shown for corresponding lines.

still be discerned, although a cube orientation is also present in the upper portion of the IPF map in Fig. 5(a) for material pressed without backpressure. It is possible that this may be an orientation from the annealed condition that was retained during the ECAP pressing. Within this region, a new orientation appears to have developed as suggested by the large orientation changes in the point-to-origin traverse shown on the right-hand side of Fig. 5(a). With backpressure during pressing, the texture includes B fiber orientations as well as the C orientation. In Fig. 5(b), long-range lattice rotations have resulted in the development of a B texture component in a band located 70–90 μm from the origin of the traverse and adjacent to a C component above and to the left of this band in the IPF map; this suggests that the accumulation of lattice rotations may lead to HAB formation as adjacent band-like regions experience rotation toward end orientations in the texture. A splitting by about 5° in both shear texture variants is also apparent in the pole figure data of Fig. 5(b). This is evidently associated with the formation of a sub-boundary (indicated by the arrows in the IPF); such a feature may be a precursor to high-angle boundary formation. The misorientation of this particular sub-boundary is ~8° as seen at the arrow in the point-to-origin traverse.

Data for material pressed through a die having a 90° relief angle is presented in Fig. 6. Distinct band-like features are apparent in the microstructures and the bands tend to be more nearly aligned with the axis of the die exit channel, especially in the first billet that experienced pressing without backpressure. The texture of the material pressed without backpressure exhibits large rotations about the flow plane normal toward the die exit channel. Indeed, comparison of the texture data to the key in Fig. 3(c) reveals that the texture of the billet pressed without backpressure in Fig. 6(a) includes of an A/B orientation that is rotated almost 90° clockwise about the flow plane normal at this location along the billet axis. A C orientation may also be discerned and it, too, is similarly rotated about the flow plane normal. Such texture rotations were especially noteworthy in billet locations that had been closest to the outer radius of the die. In contrast, the texture in the second billet, which experienced backpressure during pressing, includes both A and B fiber components that are nearly aligned with the bisector of the die channel angle. Thus, textures in materials pressed with back pressure appear to correspond closely to orientations expected from the idealized model of ECAP while textures obtained for pressing without back pressure exhibit varying rotations about the flow plane normal. Splitting of the individual texture components is again apparent in samples pressed through the die with the relief angle of 90° and this is especially evident in the sample pressed with backpressure. Individual components exhibit splitting by as much as 15°; in IPF map this is reflected in formation of bands having lattice orientations corresponding to the orientations in these split components and separated by boundaries.

Billets were repetitively pressed through four passes by route A (without rotation about the billet axis between passes) using an ECAP die having the 90° relief angle. Microstructure data and pole figures are provided in Fig. 7. The texture of first billet is shown in Fig. 7(a) and it has two components: one is a B-fiber

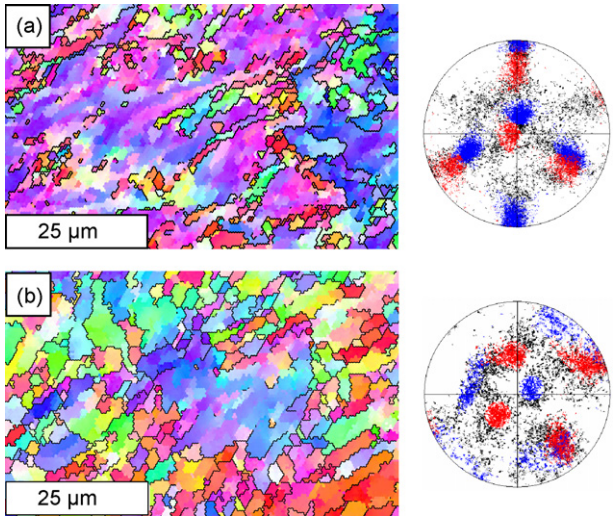

Fig. 7. Microstructure (IPF map) and (1 1 1) PFs of CP aluminum pressed four times through the die with die relief angle, $\Psi = 90^\circ$: (a) no backpressure and (b) with backpressure.

Table 1
Average (sub)grain diameter and fraction of high-angle boundaries as a function of relief angle, backpressure and number of passes

Number of passes	Relief angle (Ψ)	Average diameter (μm)		HAB fraction (%)	
		No backpressure	Backpressure	No backpressure	Backpressure
One	0	3.3	4.5	16.5	10
	45	3.5	3.7	12.6	8.4
	90	3.8	3.9	20.3	16.4
Four	90	1.2	1.1	58.2	66.5

orientation aligned with the die channel angle bisector while the second is an A/B orientation is rotated toward and aligned with die channel exit direction. The microstructure is much finer after four passes and a mean grain size of about 5 μm is apparent for both samples. However, grains up to 10 μm in size can be discerned. The texture of the billet pressed with backpressure exhibits an A/B orientation that is aligned with plane of the die channel intersection. Again, pressing with back pressure appears to suppress texture rotation and the resulting textures appear to include orientations expected from idealized ECAP. In the latter case splitting of texture components is not evident although significant broadening in the texture components is also apparent and this may mask any splitting of these components.

Table 1 summarizes the effects of die relief angle and back pressure on the (sub)grain size and the fraction of high-angle boundaries (HABs) obtained during ECAP in this study. Altogether, these data indicate that HABs comprise 10–20 pct of the boundaries while the grain size is 3–4.5 μm after one pass. When the inhomogeneous character of these microstructures is taken into account, these data indicate that neither the fraction of HABs nor the grain sizes are strongly dependent on either the die relief angle or the presence of back pressure during pressing. Data for material after four repetitive ECAP passes are compared in Table 1 to the results for material after one pass. These data show that the (sub)grain size is reduced to $\sim$1.0 μm while the fraction of HABs has increased to 55–65 pct. Thus, the predominant factor in refinement is the strain.

4. Discussion

The separate effects of backpressure and die relief angle on texture and microstructure have been evaluated for the initial ECAP pass and for material pressed through four passes by route A. Altogether, the data of this investigation show that the texture components that develop during the initial pass conform to the idealized description of ECAP, wherein shear occurs in the direction of the bisector of the die channel angle on the plane of the die channel intersection, when backpressure is superimposed during pressing. This was also observed in material pressed through four passes by route A with superimposed backpressure. In the absence of backpressure shear texture components generally exhibited rotations about the flow plane normal toward the die exit channel. Rotations of shear texture components by 20–25° were noted after pressing in a die with a relief angle $\Psi = 0°$ and rotations approaching 90° were observed in a die with inserts that provided a relief angle $\Psi = 90°$. Such rotations may reflect progressive shearing through a fan-shaped region around the plane of the die channel intersection, and shearing displacements perpendicular to as well as parallel to the plane of the die channel intersection. Splitting of variants of a B fiber component was noted in samples pressed with backpressure while the A/B shear texture component was more commonly observed in samples pressed without backpressure. Despite the effects on texture neither backpressure nor die relief angle affected the (sub)grain size and fraction of HABs in this material.

Segal [16] has shown that die wall friction and strain hardening of the billet material lead to formation of a dead zone at the outer corner of the die due to constraint effects. The presence of non-deforming material in the dead zone induces progressive shearing of the billet throughout a fan-shaped region surrounding the plane of the die channel intersection. Then, shearing displacements take place perpendicular to as well as parallel to the plane of the die channel intersection and result in a resolved shear that is rotated about the flow plane normal toward the axis of the die exit channel. The introduction of a relief angle at the outer corner of the die channel intersection will give this same effect [16] (Fig. 1). With the superposition of backpressure shear textures align more nearly with the shear plane of the die, suggesting that backpressure suppresses progressive shearing during ECAP. A review of the literature suggests that the effect of backpressure during ECAP has been examined in only a few publications [6,7]. Nevertheless, it is apparent that the application of progressively increasing backpressure (e.g., by use of a separate plunger in the die exit channel) would cause plastic deformation to cease if the applied backpressure were to become equal to the forward pressure in the die entrance channel because shear stresses would be reduced to zero throughout the billet. A further increase in backpressure would result in a reversal of the sense of deformation and a corresponding reversal in the sense of shear in the region of the die channel intersection. Altogether, this is consistent with the observation in Figs. 4–6 that shear texture components tend to align with the bisector of the die channel angle on the plane of the die channel intersection with the application of backpressure during ECAP. That is, the backpressure suppresses the rotation of the resolve shear toward the axis of the die exit channel.

Following Segal [16], the progressive deformation as the billet passes through the fan-shaped region surrounding the die channel intersection during an ECAP pass is illustrated in schematic of Fig. 8(a). This region reflects dead zone formation at the outer corner of the die channel intersection due to constraint effects. The details of its size and shape reflect factors, such as wall friction, the constitutive behavior of the billet material and features of the die design, such as the presence of

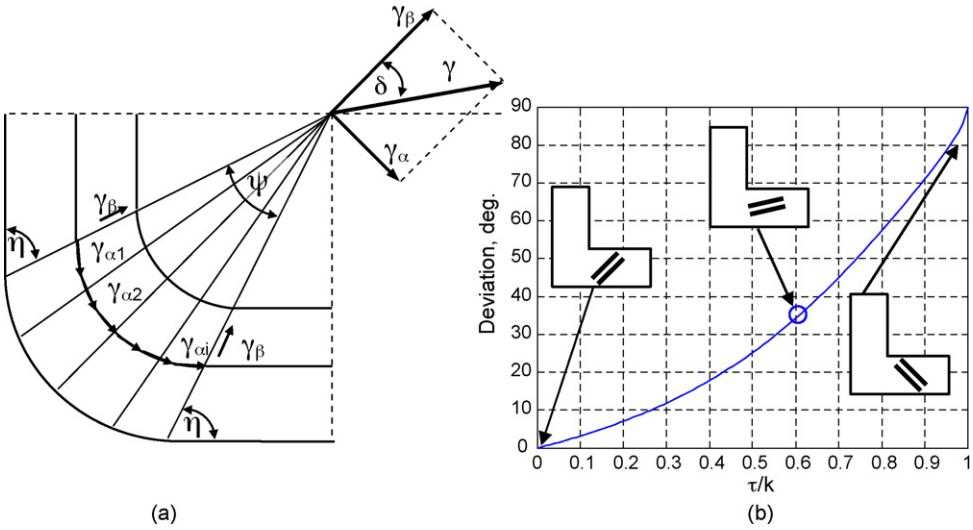

Fig. 8. A schematic representation of the shearing displacements in Segal's slip line analysis of progressive deformation through a fan-shaped region at the die channel intersection is shown in (a) while the deviation angle, δ, as a function of the ratio of shear yield stress to friction stress, τ/k, is plotted in (b).

a relief angle at the outer corner of the die channel intersection. Segal [16–18] has considered the role of die wall friction and utilized slip line methods to analyze flow of material through an ECAP die. The analysis demonstrated that the total shear may be decomposed into shears involving displacements along the β slip lines as the billet enters and leaves the fan region, and progressive shearing along the α slip lines as the billet passes through the fan region. These slip lines and displacements are depicted in Fig. 8(a). Shearing displacements along the β slip lines give a resultant shear

$$\gamma_\beta = 2\,\cot(\eta)\cos\left(\frac{\Psi}{2}\right), \tag{1}$$

where η is the angle between the β slip line and the die wall and Ψ is the angle subtended by the fan. In turn, the angle η is given by

$$\eta = \frac{\pi}{2} - \frac{1}{2}\arccos\left(\frac{\tau}{k}\right), \tag{2}$$

where τ/k is the ratio of the friction stress, τ, to the material's shear yield strength, k. The friction stress, τ, is the product of the friction coefficient and the normal stress acting at the die wall. The value of τ/k may also reflect constraint effects and their influence on plastic flow in and through the dead zone at the outer corner of the die channel intersection. The resultant shear γ_β is aligned with the trace of plane of the die channel intersection, i.e., the bisector of the die channel angle. Progressive shearing displacements along the α slip lines give a resultant shear

$$\gamma_\alpha = \Psi, \tag{3}$$

which is perpendicular to the plane of the die channel intersection. The total shear, γ, will be the sum of γ_β and γ_α, as illustrated at the upper right in Fig. 7(a), and this will be inclined at an angle, δ, the bisector of the die channel angle and given by

$$\delta = \arctan\left(\frac{\gamma_\alpha}{\gamma_\beta}\right). \tag{4}$$

In the absence of friction, the fan angle $\Psi \to 0$ and $\eta \to 45^\circ$; then, $\gamma \to \gamma_\beta$, and $\delta \to 0^\circ$, which corresponds to the idealized description of frictionless straining during an ECAP pass. Again, following Segal [16], when die wall friction and constraint effects predominate during deformation then the fan angle $\Psi \to 90^\circ$ and $\eta \to 90^\circ$; furthermore, $\gamma \to \gamma_\alpha$ and, in such a circumstance, $\delta \to 90^\circ$.

As an extension of Segal's slip line analysis [16–18], measured ECAP textures expressed in the flow plane for as-pressed samples would be expected to exhibit shear texture components in which the apparent SD would be rotated about the flow plane normal, i.e., the z-axis in Fig. 1, toward the axis of the die exit channel. Bowen et al. [19], Gholinia et al. [9] and Beyerlein and Tomé [20] have also observed such texture rotations and these authors have discussed them mainly in terms of the effects of friction. The extent of such rotation will depend on constraint effects as well as friction, and the effects of these factors may be approximated using Eq. (4), as shown in Fig. 8(b) wherein the deviation angle, δ, is plotted as a function of Segal's parameter τ/k. When $\tau/k = 0$, the deviation angle is 0° and the shear plane and SD coincide with the die channel intersection, i.e., idealized, frictionless ECAP confined to the plane of the die channel intersection as indicated in the inset diagram. As the ratio τ/k increases, the deviation angle will also increase and this reflects increasing hydrostatic constraint effect and dead zone formation with progressive shearing through a fan-shaped region subtending a fan angle, Ψ, at the outer corner of the die due to the effects of die wall friction. As an example, a 35° rotation of the shear plane and SD toward the die channel intersection corresponds to a ratio $\tau/k \sim 0.6$. It has recently been pointed out [21] that the introduction of a relief angle at the outer corner of the die channel intersection leads to an increase in the fan angle, Ψ,

and this is, in effect, equivalent to an increase in the ratio τ/k. Thus, the rotation observed here in the absence of backpressure reflects the introduction of a relief angle in the die in addition to the effects of friction in the ECAP die.

Recent publications [6,7] have highlighted the benefit of controllable backpressure and shown its positive effect upon workability and grain refinement as well as on post-processing fatigue behavior of Al-alloys. Among other effects, superimposed hydrostatic pressure will suppress crack initiation and also results in improved homogeneity of billet microstructures. Finally, the application of backpressure appears to induce splitting in the orientation variants of the shear texture components that form during pressing (e.g., Figs. 4–6). It has recently been suggested [22] that high-angle boundaries develop from band-like structures having lattice orientations that correspond to symmetrically equivalent orientations in the texture. In Fig. 5(b) a boundary (delineated by the arrows) has a misorientation of 5–15°, as indicated in the point-to-origin misorientation profile along the indicated traverse. The lattice orientations on opposite sides of the boundary are apparently associated with the splitting of a B fiber $\{1\,1\,2\}\langle 1\,1\,0\rangle$ component in the texture. Such splitting may be associated with band formation and thus may be a precursor to formation of high-angle boundaries; this phenomenon appears to be more prominent and splitting of up to 15–20° became apparent for pressing accomplished under backpressure and as die relief angle increased up to 90° (e.g., Fig. 5). Nevertheless, the population of HABs appeared to increase mainly as a function of strain and not as a function of either backpressure or die relief angle. With increasing of number of passes, Fig. 7(b), the splitting of texture components is no longer evident although the phenomenon may be masked by the randomizing of the texture.

5. Concluding remarks

1. Detailed study of ECAP aluminum of commercial purity has been performed by OIM after the initial pressing pass and after four passes by route A.
2. Significant refinement of microstructure has been achieved irrespective of die channel geometry and backpressure.
3. In general, texture components correspond to those expected for idealized ECAP. However, for ECAP with $2\theta = 90°$ and $\Psi = 90°$, shear texture components corresponding to progressive shear along the periphery of a fan-shaped region may be detected, especially for pressing in the absence of backpressure.
4. Texture data for materials pressed with backpressure corresponds more closely with the idealized model of ECAP involving shear on the plane of the die channel intersection and this indicates that backpressure tends to suppress progressive shear along the periphery of the fan created by the die relief angle.
5. Repetitive ECAP leads to microstructure refinement and increased populations of HABs.
6. Significant splitting of shear texture components has been detected during the initial ECAP pass. This splitting appears in the microstructure as bands separated by sub-boundaries. With increasing die relief angle the splitting becomes more prominent and may lead to formation of high-angle boundaries.
7. HAB fractions after one pass were in range of 10–20% for all cases examined.
8. Strain is the predominant factor in refining the grain size and increasing the fraction of HABs during repetitive ECAP.

Acknowledgements

This work was partially supported by INTAS-03513779 and RFBR-05-03-32233-a. One of the authors (A.P.Z.) thanks the National Research Council of the National Academy of Science (USA) and the Spanish Ministry of Education and Science (under Ramón y Cajal program) for financial support. Another author (T.R.M.) was partially supported by the US Air Force Office of Scientific Research under funding document no. F1ATA06058G001.

References

[1] Z. Horita (Ed.), Mater. Sci. Forum 503–504 (2005) 1030.
[2] N.A. Smirnova, V.I. Levit, V.I. Pilyugin, R.I. Kuznetsov, L.S. Davydova, V.A. Sazonova, Fiz. Met. Metalloved. 61 (1986) 1170.
[3] Y. Saito, H. Utsunomiya, N. Tsuji, T. Sakai, Acta Mater. 47 (1999) 579.
[4] K. Oh-ishi, T.R. McNelley, Metall. Mater. Trans. 35A (2004) 2951.
[5] V.M. Segal, V.I. Reznikov, A.E. Drobyshevskiy, V.I. Kopylov, Russ. Metall. 1 (1981) 99.
[6] V.V. Stolyarov, R. Lapovok, J. Alloys Compd. 378 (2004) 273.
[7] V.V. Stolyarov, R. Lapovok, I.G. Brodova, P.F. Thomson, Mater. Sci. Eng. A 357 (2003) 159.
[8] T.R. McNelley, D.L. Swisher, in: Y.T. Zhu, T.G. Langdon, R.Z. Valiev, S.L. Semiatin, D.H. Shin, T.C. Lowe (Eds.), Ultrafine Grained Materials III, TMS, Warrendale, PA, 2004, p. 89.
[9] A. Gholinia, P. Bate, P.B. Prangnell, Acta Mater. 50 (2002) 2121.
[10] L.S. Tóth, R.A. Massion, L. Germain, S.C. Baik, S. Suwas, Acta Mater. 52 (2004) 1885.
[11] A.P. Zhilyaev, K. Oh-ishi, T.G. Langdon, T.R. McNelley, Mater. Sci. Eng. A 410–411 (2005) 277.
[12] OIM User's Manual, EDAX-TSL, E. Mahway, NJ, 2005.
[13] S.D. Terhune, D.L. Swisher, K. Oh-ishi, Z. Horita, T.G. Langdon, T.R. McNelley, Metall. Trans. 33A (2002) 2173.
[14] G.R. Canova, U.F. Kochs, J. Jonas, Acta Metall. 32 (1984) 211.
[15] F. Montheillet, M. Cohen, J. Jonas, Acta Metall. 32 (1984) 2077.
[16] V.M. Segal, Mater. Sci. Eng. A 345 (2003) 36.
[17] V.M. Segal, Mater. Sci. Eng. A271 (1999) 322.
[18] V.M. Segal, Mater. Sci. Eng. A338 (2002) 331.
[19] J.R. Bowen, A. Gholinia, S.M. Roberts, P.B. Prangnell, Mater. Sci. Eng. A287 (2000) 87.
[20] I.J. Beyerlein, C.N. Tomé, Mater. Sci. Eng. A380 (2004) 171.
[21] S. Li, M.A.M. Bourke, I.J. Beyerlein, D.J. Alexander, B. Clausen, Mater. Sci. Eng. A382 (2004) 217.
[22] A.P. Zhilyaev, D.L. Swisher, K. Oh-ishi, T.G. Langdon, T.R. McNelley, Mater. Sci. Eng. A 429 (2006) 137.